The Canadian Mineralogist
Vol. 43, pp. 1457-1468 (2005)

WILUITE FROM ARICCIA, LATIUM, ITALY: OCCURRENCE AND CRYSTAL STRUCTURE

FABIO BELLATRECCIA

Dipartimento di Scienze della Terra, Università di Roma "La Sapienza", Piazzale Aldo Moro 5, I–00185 Roma, Italy, and Dipartimento di Scienze Geologiche, Università Roma Tre, Largo S. Leonardo Murialdo 1, I–00146 Roma, Italy

FERNANDO CÁMARA AND LUISA OTTOLINI

CNR – Istituto di Geoscienze e Georisorse, Sede di Pavia, via Ferrata 1, I–27100 Pavia, Italy

GIANCARLO DELLA VENTURA§, GIANNANTONIO CIBIN AND ANNIBALE MOTTANA

Dipartimento di Scienze Geologiche, Università Roma Tre, Largo S. Leonardo Murialdo 1, I–00146 Roma, Italy

ABSTRACT

We report a new occurrence of the rare mineral wiluite, the B-rich equivalent of vesuvianite, from Ariccia, Alban Hills volcano, Rome, Italy. The specimen studied was found in the collection of the Museum of Mineralogy of the University of Rome (label MMUR22496/482). Wiluite from Ariccia was sampled at the Parco Chigi quarry, within the phreatomagmatic unit emitted by the Albano maar known locally as "Peperino di Marino". It occurs as dark brown to black euhedral, well-formed prismatic crystals, up to 1.0 cm in length and 0.5 cm across. Optical observations show a weak pleochroism and an imperfect extinction. The mineral is uniaxial (+) with ω 1.722(2) and ε 1.727(2). It is tetragonal *P*4/*nnc*, *a* 15.716(2), *c* 11.704(2) Å, *V* 2890.8(7) Å^3. The crystal-chemical formula, obtained by combining EMP, SIMS and XREF data and calculated on the basis of 18 Si atoms, is: $^{X}(Ca_{18.72}Mg_{0.15}Sr_{0.02}La_{0.05}Ce_{0.04}Nd_{0.01})$ $^{Y(1)}(Fe^{3+}_{0.36}Mg_{0.26}Ti_{0.27}Mn_{0.11})$ $^{Y(2)}(Al_{3.67}Fe^{3+}_{0.19}Mg_{0.14})$ $^{Y(3)}(Al_{3.29}Fe^{3+}_{1.36}Mg_{3.35})$ $^{T(1)}(B_{2.18}Al_{0.02}Be_{0.02}H_{0.47}\square_{1.31})$ $^{T(2)}(B_{0.68}H_{0.32})$ $^{Z}Si_{18}O_{68}$ $^{O(11)}(F_{1.21}O_{6.79})$ $^{[O(10)+O(12)]}O_{2.68}$. The micro OH-stretching FTIR spectrum consists of a defined triplet of broad bands at 3639, 3573 and 3488 cm^{-1}, respectively, and a very broad, composite absorption at 3300 cm^{-1}. All bands are strongly polarized, with maximum absorption for **E** // *c* and minimum absorption for **E** $\perp$ *c*. The integrated molar absorption coefficient for wiluite is ε_i = 90.000 ± 1500 l mol^{-1} cm^{-2}. In the 1600–1100 cm^{-1} region, absorptions due to both $^{[3]}$B–O and $^{[4]}$B–O bonds are observed. The Mg and Al *K*-edge X-ray-absorption spectra are consistent with the presence of two octahedral coordination sites for both atoms, as determined by XREF, with the addition of a third, highly unusual, five-fold pyramidal site for the divalent cation.

Keywords: wiluite, vesuvianite, electron-microprobe data, secondary-ion mass spectrometry, infrared spectroscopy, single-crystal X-ray diffraction, boron, Ariccia, Italy.

SOMMAIRE

Nous décrivons un nouvel exemple de la wiluite, espèce rare, l'analogue riche en bore de la vésuvianite, provenant d'Ariccia, volcan des collines albanes, à Rome, en Italie. L'échantillon a été trouvé dans la collection du Musée de Minéralogie de l'Université de Rome (numéro MMUR22496/482). Cet échantillon provient de la carrière de Parco Chigi, de l'unité phréatomagmatique émise par le maar de Albano, appelée localement "Peperino di Marino". La wiluite y est présente en cristaux prismatiques idiomorphes bruns foncés à noirs, atteignant 1.0 cm de long et 0.5 cm de diamètre. Les observations optiques révèlent un faible pléochroïsme et une extinction imparfaite. Le minéral est uniaxe (+), avec ω 1.722(2) et ε 1.727(2). Il est tétragonal *P*4/*nnc*, *a* 15.716(2), *c* 11.704(2) Å, *V* 2890.8(7) Å^3. La formule cristallochimique, obtenue à la lumière des données obtenues avec une microsonde électronique, une microsonde ionique et par diffraction X sur monocristal, et recalculées sur une base de 18 atomes de Si, serait: $^{X}(Ca_{18.72}Mg_{0.15}Sr_{0.02}La_{0.05}Ce_{0.04}Nd_{0.01})$ $^{Y(1)}(Fe^{3+}_{0.36}Mg_{0.26}Ti_{0.27}Mn_{0.11})$ $^{Y(2)}(Al_{3.67}Fe^{3+}_{0.19}Mg_{0.14})$ $^{Y(3)}(Al_{3.29}Fe^{3+}_{1.36}Mg_{3.35})$ $^{T(1)}(B_{2.18}Al_{0.02}Be_{0.02}H_{0.47}\square_{1.31})$ $^{T(2)}(B_{0.68}H_{0.32})$ $^{Z}Si_{18}O_{68}$ $^{O(11)}(F_{1.21}O_{6.79})$ $^{[O(10)+O(12)]}O_{2.68}$. La microspectrométrie infrarouge de la zone d'étirement de OH avec transformation de Fourier révèle un trio de bandes floues, à 3639, 3573 et 3488 cm^{-1}, respectivement, et une absorption composite très floue à 3300 cm^{-1}. Toutes ces bandes sont fortement polarisées, avec une absorption maximum pour **E** // *c* et une absorption minimum pour **E** $\perp$ *c*. Le coefficient d'absorption molaire intégré de la wiluite ε_i serait 90.000 ± 1500 l mol^{-1} cm^{-2}. Des absorptions dues aux liaisons $^{[3]}$B–O et $^{[4]}$B–O sont présentes entre 1600 et 1100 cm^{-1}. Les

§ *E-mail address*: dellaven@uniroma3.it

spectres d'absorption des rayons X émis par Mg et Al concordent avec la présence de deux sites à coordinence octaèdrique pour chaque atome, tel qu'indiqué par affinement de la structure, et aussi la présence d'un troisième site très inhabituel à coordinence cinq, pyramidal, pour le cation bivalent.

(Traduit par la Rédaction)

Mots-clés: wiluite, vésuvianite, microsonde électronique, microsonde ionique, spectroscopie infrarouge, diffraction X sur monocristal, bore, Ariccia, Italie.

Introduction

Wiluite, $Ca_{19}(Al,Mg,Fe,Ti)_{13}(B,Al,\square)_5Si_{18}O_{68}(O,OH)_{10}$, is the B-rich analogue of vesuvianite, recently characterized from a sample of Wilui River, Sakha Republic, Russian Federation, and found within serpentinite associated with grossular and serpentine-group minerals. Although it has been known for some time that vesuvianite commonly contains boron and that vesuvianite from the Wilui region, in particular, contains significant amounts of boron (indeed, the name wiluite had been in use in the literature for samples from there for a long time), the species had never been formally defined until the work of Groat *et al*. (1998). As shown by Groat *et al*. (1994) vesuvianite can incorporate up to 4 wt% B_2O_3, the boron substitutes for H, according to the $BMgH_{-2}Al_{-1}$ exchange vector. Boron is distributed over two sites of the vesuvianite structure: *T*(1), where it replaces two H1 hydrogen atoms and adopts tetrahedral coordination, and *T*(2), where it replaces one H2 hydrogen atom and adopts triangular coordination (Groat *et al*. 1994, 1996).

During a systematic crystal-chemical study of vesuvianite-group minerals (Bellatreccia 2003) collected in the tephra scattered within the Plio-Pleistocene volcanic region of Latium, Italy, we found that most of the samples studied contain significant boron, and one sample in particular has B >> 0.25 atoms per formula unit (*apfu*), thus allowing it to be classified as wiluite. Wiluite is a very rare mineral and has been so far reported only from three localities in the world (Groat *et al*. 1998): 1) Wilui River, Sakha Republic, Russian Federation, 2) Templeton Township, Quebec, Canada, and 3) Bill Waley mine, Tulare County, California, USA. Here, we report on the crystal-chemical study of wiluite from Ariccia, Latium, Italy, a new occurrence. We emphasize that the high B content of vesuvianite-group minerals from Alban Hills, and from the Ariccia quarry in particular, had previously been noted (A. Taddeucci, pers. commun.); however, the data were never published.

Occurrence, Physical and Optical Properties

The crystal chosen for study is from the collection housed in the Museum of Mineralogy of the University of Rome "La Sapienza" (label MMUR 22496/482, hereafter 26FB). It was collected at the ignimbrite quarry of Parco Chigi, Ariccia community, Rome, Latium. The phreatomagmatic unit in which wiluite occurs, locally known as "Peperino di Marino", erupted about 23,000 years ago from the polygenetic Lake Albano maar, part of the Alban Hills volcano in central Italy (Giordano *et al*. 2002). In Latium, vesuvianite typically occurs in skarn-type ejecta (Bellatreccia 2003), which are fragments of the metasomatized carbonate-rich wallrock. Wiluite from Parco Chigi is found scattered within the pyroclastic deposit; as such, it is unclear whether it originated from disaggregated metasomatic xenoliths or by magmatic crystallization.

Wiluite occurs as well-formed, euhedral, prismatic crystals (Fig. 1), with a maximum dimension of 1.0 cm along *c* and 0.5 cm across. All crystals show a well-defined morphology, with a short prismatic habit; they consist of tetragonal {100} and {110} prisms doubly terminated by ditetragonal {101} pyramids cut at the apex by the {001} pinacoid. They are dark brown to black in hand specimen. In thin section, the mineral is colorless to light yellowish green, very weakly pleochroic. There is a strong optical sector-zoning, from cross-hatched domains to fine lamellar zones; under crossed polarizers, the extinction is never perfect. The indices of refraction were measured on a single polished surface of more than 1 mm^2 using a jeweller's refractometer in monochromatic light (590 nm), with an accuracy of about 0.002 (Hurlbut 1984). Wiluite from Ariccia is uniaxial (+), with ω 1.722(2) and ε 1.727(2). Vesuvianite is an optically negative mineral (Deer *et al*. 1982); however, B-rich vesuvianite (and wiluite) are invariably positive (Groat *et al*. 1992, 1998). Borovikova *et al*. (2003) recently revised the optical characteristics of a large number of samples and concluded that, among the B-rich (low- and high-symmetry) vesuvianite samples, those containing $^{[3]}B$ are negative, whereas those containing $^{[4]}B$ are positive. Owing to the mixed occupancy of the *T* sites, the actual distribution of boron between sites and the coordination of B are not easy to obtain directly with X-ray methods. This information, however, is provided, at least qualitatively, by IR spectroscopy in the B–O stretching region (1200–1000 cm^{-1}). Powder and single-crystal spectra (see below) of wiluite from Ariccia show absorptions due to both $[BO_3]^{3-}$ and $[BO_4]^{5-}$ groups. Therefore, it

is unclear whether the optical sign of vesuvianite is indeed directly linked to the coordination of B in the structure.

Chemical Composition

Wavelength-dispersion (WD) analysis of the sample for the main and trace constituents was done using a Cameca SX50 electron microprobe at the CNR – Istituto di Geologia Ambientale e Geoingegneria (IGAG), Università di Roma "La Sapienza". Analytical conditions were 15 kV (accelerating voltage) and 15 nA (beam current), with a 5 μm beam diameter. Counting time was 20 s on both peak and background. We used the following standards: wollastonite (Si*K*α, TAP; Ca*K*α, PET), periclase (Mg*K*α, TAP), corundum (Al*K*α, TAP), magnetite (Fe*K*α, LIF), rutile (Ti*K*α, LIF), Mn metal (Mn*K*α, LIF). Analytical errors are 1% relative for major elements and 5% relative for trace elements. Data reduction was done by the PAP method (Pouchou & Pichoir 1985).

We established the concentrations of the light elements, Y, Sr, and the rare-earth elements (REE) on the same mount by secondary-ion mass spectrometry (SIMS) using an ion microprobe (Cameca IMS 4f) at CNR – Istituto di Geoscienze and Georisorse (IGG), Università di Pavia. A $^{16}O^-$ primary ion beam accelerated at 12.5 kV, with a beam intensity of 3 nA and a beam diameter ≤5 μm, was employed. The CaO content (wt%), derived by electron-microprobe analysis, was used as the internal reference for Y, Sr and the REE, whereas the SiO_2 content (wt%) was selected for H, Li, Be and B. Both CaO and SiO_2 were used in the quantification of levels of F, U and Th (Ottolini & Oberti 2000). We used as standards the Snarum and Durango apatites for the REE, Y and Sr, BB and LL Std b glasses for U and Th, and danalite for Be. For the calibration of H, Li and B, low-Si silicate standards were used (see Ottolini *et al*. 2002 for details). The analytical accuracy is estimated to be 10% relative for H and F, and close to 5% relative for Li, Be and B. For the heavier elements, the relative uncertainty is discussed in detail in Ottolini & Oberti (2000).

The overall composition of the wiluite from Ariccia, obtained by combining EMPA (Si, Al, Mg, Ca, Fe, Ti and Mn) and SIMS data (H, Li, Be, B, F, Y, REE, Th, U and Sr), is reported in Table 1. The crystal-chemical formula is based on 18 Si atoms, thus excluding Al from the Z sites, in agreement with the standard formula suggested by Groat *et al*. (1996); this procedure is also supported by our XANES results (see below). Wiluite from Ariccia has a composition very similar to wiluite from the Sakha Republic (Groat *et al*. 1998), the only notable difference being the significantly higher B and F contents. The chondrite-normalized REE pattern (REE_{cn}) of this sample of wiluite (Fig. 2) is broadly similar to the patterns displayed by most minerals from the volcanic ejecta of Latium (Della Ventura *et al*. 1993, 1996, 1999, Oberti *et al*. 1999, Ottolini & Oberti 2000). It shows a significant enrichment in the light rare-earth elements (LREE) and a linear decrease toward the heavy rare-earth elements (HREE). An interesting feature arises when comparing the REE_{cn} pattern of the sample studied with the patterns of lavas or volcanic ejecta from the same locality (Fig. 2). Wiluite shows a strong enrichment in the LREE relative to the host rock, and a significant depletion in the HREE. This behavior suggests that vesuvianite-group minerals have a definite preference for LREE over HREE. For a sample from San Benito County, California, Fitzgerald *et al*. (1987) reported a total REE content of 14.74 wt%, the chondrite-normalized pattern of which (not shown in Fig. 2) is identical to the pattern of our sample of wiluite. However, this point cannot be definitively evaluated because, in the mineralogical literature, REE data on vesuvianite-group minerals are rare and incomplete.

Crystal Structure

Experimental

A crystal of 0.23 × 0.22 × 0.20 mm was selected for X-ray data collection on the basis of its sharp extinction.

TABLE 1. CHEMICAL COMPOSITION AND UNIT FORMULA OF WILUITE FROM ARICCIA, LATIUM, ITALY

	Mean *n* = 4	Compositional range *n* = 26		Number of atoms	
SiO_2 wt%	36.33	36.66	33.78	Si *apfu*	18.00
Al_2O_3	11.97	12.88	10.50	Al	6.97
MgO	5.27	5.70	3.92	Mg	3.75
CaO	35.26	35.84	33.52	Fe	1.91
TiO_2	0.71	1.43	0.58	Ti	0.27
MnO	0.27	0.35	0.00	Mn	0.11
Fe_2O_3	5.11	7.89	5.01	Σ*Y*	13.00
SrO	0.079	0.081	0.077	Ca	18.72
Y_2O_3	0.003	0.004	0.003	Mg	0.15
La_2O_3	0.298	0.500	0.097	Sr	0.023
Ce_2O_3	0.235	0.376	0.095	Y	0.001
Pr_2O_3	0.014	0.020	0.008	La	0.054
Nd_2O_3	0.034	0.043	0.025	Ce	0.043
Sm_2O_3	0.003	0.004	0.003	Pr	0.003
Eu_2O_3	0.000	0.001	0.000	Nd	0.006
Gd_2O_3	0.003	0.003	0.002	Sm	0.001
Dy_2O_3	0.001	0.001	0.001	Eu	0.000
Er_2O_3	0.000	0.000	0.000	Gd	0.000
Yb_2O_3	0.000	0.000	0.000	Dy	0.000
UO_2	0.001	0.001	0.000	Er	0.000
ThO_2	0.002	0.004	0.001	Yb	0.000
B_2O_3	3.350	3.89	3.35	U	0.000
BeO	0.016	0.018	0.014	Th	0.000
Li_2O	0.001	0.001	0.001	Σ*X*	19.00
F	0.774	0.775	0.774		
H_2O	0.239	0.258	0.220	B	2.86
				Be	0.02
Subtotal	99.97			Li	0.00
O=F	0.33			Al	0.02
				H	0.79
Total	99.64			□	1.31
				Σ*T*	5.00
				F	1.21

The unit formula, in atoms per formula unit (*apfu*), is based in 18 atoms of Si. The compositional range was defined on a second crystal of wiluite. Total iron is expressed as Fe_2O_3. The data for the first seven constituents were obtained by electron-microprobe analysis; the rest were obtained by secondary ion mass spectrometry (SIMS).

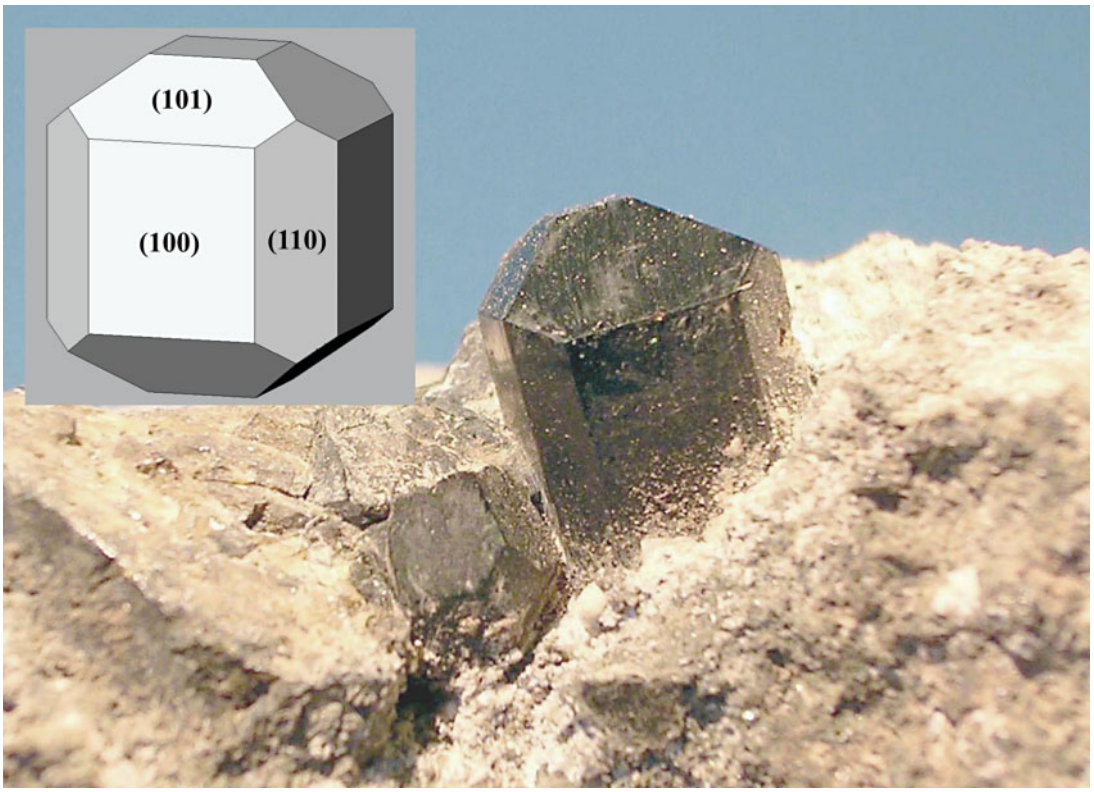

FIG. 1. Crystal habit of wiluite from Ariccia; width of field of view: 5 cm.

Diffracted intensities were recorded using a single-crystal Nonius Kappa CCD diffractometer at the Institut für Mineralogie und Kristallographie, Geozentrum, Universität Wien (Austria) with a Mo$K\alpha$ (λ = 0.71073 Å) sealed tube. The crystal-to-detector distance was 28 mm. A total of 406 images were recorded by φ- and ω-rotations of 2° in eight sets of images. Integration time for each frame was 65 s. Intensity data were extracted from images using the DENZO–SMN software package (Otwinowski & Minor 1997). Data were corrected for Lorentz, polarization and background. An empirical "multi-scan" absorption correction was applied (Otwinowski & Minor 1997). Unit-cell parameters were obtained by refining the position of all the integrated intensities.

The wiluite from Ariccia is tetragonal, space group *P*4/*nnc*, as indicated by the limited number (16 out of 2339) and the very weak intensity of reflections violating the extinction conditions ($<I/\sigma(I)> < 1$). Atom coordinates published by Groat *et al*. (1996) for a specimen of vesuvianite from the Bill Waley mine, Tulare County, California (sample V56 of Groat *et al*. 1992), having a very similar chemical composition (except for B content) were used as starting parameters for the structure refinement.

Weighted full-matrix least-square refinements were completed using SHELX–97 (Sheldrick 1997). Scattering factors were taken from International Tables for X-ray Crystallography (Hahn 1995, Wilson 1995). The weighting scheme was $w = [\sigma^2(F_o^2) + (a*P)^2 + b*P]$ where $P = [0.3333 * \text{max. of } (0 \text{ or } F_o^2) + (1 - 0.3333) * F_c]$. Refinement parameters are given in Table 2, and atom coordinates and thermal displacement parameters, in Table 3, whereas in Table 4, we list selected bond-lengths and angles. Observed and calculated structure-factors are reported in Table 5, which may be obtained from the Depository of Unpublished Data, CISTI, National Research Council of Canada, Ottawa, Ontario K1A 0S2, Canada.

Site assignment

Site assignment (Table 6) have been calculated by comparing refined site-scattering values (Table 3), results of EMPA + SIMS chemical analyses normalized on the basis of 18 Si *apfu* (Table 1), and observed mean bond-lengths (Table 4). The REE are ordered at *X*(3);

calculated site-scattering values (163.3 electrons per formula unit, *epfu*) are in agreement with the observed values at the *X*(3) site (Table 3).

Scattering curves for Al^{3+} and Fe^{3+} were used to refine the site-occupancy factor (s.o.f.) of the octahedrally coordinated Y(2) and *Y*(3) sites. The observed site-scattering values (54.7 *epfu*, *i.e.*, 13.7 electrons per site) and mean bond-lengths (<*Y*(2)–*O*,*O*(11*A*)> = 1.900 Å and <*Y*(2)–*O*,*O*(11*B*)> = 1.943 Å) are compatible with almost full occupancy of Al at *Y*(2), whereas significant $Al(Fe^{3+},Mg)_{-1}$ substitution must occur at the *Y*(3) site (20.3 electrons per site; <*Y*(3)–*O*,*O*(11*A*)> = 1.994 Å and <*Y*(3)–*O*,*O*(11*B*)> = 2.013 Å). The *Y*(1) site has five-fold coordination and can be occupied by variable amounts of Al, Fe^{3+}, Mg, Ti and Mn. In our model, we used the scattering curve of Fe^{3+}, leaving the site-occupancy factor at this site free to vary. Because the distance between the *Y*(1) and *X*(4) sites along the channels parallel to the *c* axis is only 1.022 Å, only half occupancy is possible for *Y*(l). Groat *et al*. (1994) refined split positions at the *O*(10) and *Y*(1) sites to account for the large RMS displacement observed at these two sites. We also observe large values of the atom-displacement parameter at these sites, but a test to split both atom positions yielded an unstable refinement. Therefore, the observed values of the atom- displacement parameter can be interpreted as due to the variable occupancy of the *Y*(1) sites by various cations. In fact, the refined site-scattering value at the *Y*(1) site (21.7 *epfu*, Table 3) and mean bond-length (<*Y*(1)–*O*> = 2.090 Å) are compatible with its alternate occupancy by small high-charge Fe^{3+} (Ti^{4+}) cations and larger low-charge Mg (Mn^{2+}) cations, whereas Al can be excluded owing to its short ionic radius that makes it incompatible with the observed mean bond-length for *Y*(1).

In B-rich vesuvianite and wiluite, B is ordered at the T(1) and *T*(2) cavities (Groat *et al*. 1994, 1996, 1998). We refined the site occupancy and anisotropic displacement parameters at the *T*(1) site. Boron occurs at the *T*(1) cavity in tetrahedral coordination with two oxygen atoms at the *O*(7) sites and two anions at the *O*(11) sites. The refinement showed high values of the atom-displa-

TABLE 2. CRYSTAL AND STRUCTURE-REFINEMENT DATA FOR WILUITE FROM ARICCIA, LATIUM, ITALY

Wavelength	0.71073 Å
Crystal system	Tetragonal
Space group	*P*4/*nnc*
Unit-cell dimensions	*a*, *b* 15.716(2) Å
	c 11.704(2) Å
Volume	*V* 2890.8(7) Å^3
Z	2
Density (calculated)	3.403 g/cm^3
Mean *n*	1.724
Compatibility index	-0.024 (excellent)
F(000)	2979
Crystal size	0.23 × 0.22 × 0.20 mm^3
Theta range for data collection	2.17 to 33.72°
Index ranges	$-24 \le h \le 24$, $-17 \le k \le 17$, $-17 \le l \le 18$
Reflections collected	10637
Independent reflections	2898 [R(int) = 0.0242]
Completeness to theta = 33.72°	99.8%
Refinement method	Full-matrix least-squares on F^2
Data / restraints / parameters	2898 / 8 / 193
Goodness-of-fit on F^2	1.068
Final *R* indices [I > 2σ(I)]	$R1 = 0.0241$, $wR^2 = 0.0534$
R indices (all data)	$R1 = 0.0343$, $wR^2 = 0.0568$
Extinction coefficient	0.00096(10)
Largest diff. peak and hole	0.640 and -0.473 *e*.Å^{-3}

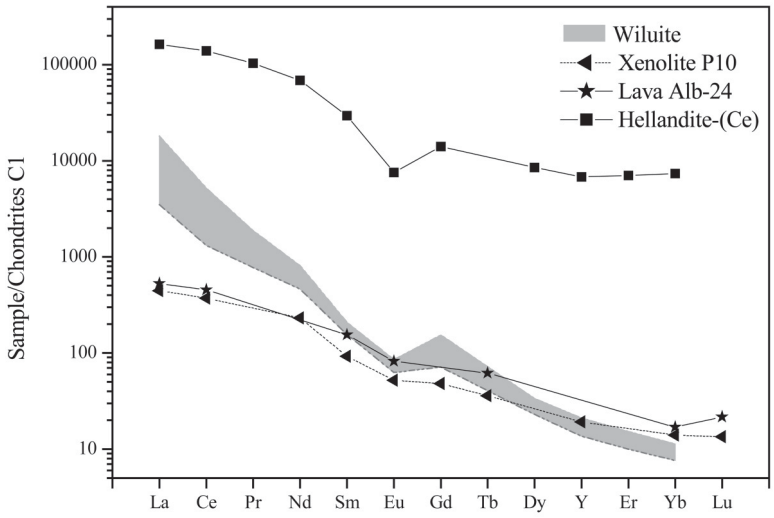

FIG. 2. Chondrite-normalized REE pattern of the wiluite compared with that of the volcanic rocks from the Alban Hills (Federico *et al*. 1994, Peccerillo *et al*. 1984) and hellandite-(Ce) (Oberti *et al*. 1999). REE normalization-factors are based on chondrite C1, from Anders & Ebihara (1982).

TABLE 3. FRACTIONAL ATOM COORDINATES AND ANISOTROPIC DISPLACEMENT PARAMETERS FOR WILUITE FROM ARICCIA LATIUM, ITALY

	ss[b]	x/a	y/b	z/c	U_{eq}	[a]U_{11}	U_{22}	U_{33}	U_{12}	U_{13}	U_{23}
Z(1)	28	¾	¼	0	0.0069(1)	0.0075(2)	0.0075(2)	0.0056(3)	0	0	0
Z(2)	112	-0.17859(2)	0.04304(2)	0.87208(3)	0.0099(1)	0.0096(2)	0.0129(2)	0.0073(2)	0.0017(1)	-0.0006(1)	0.0018(1)
Z(3)	112	-0.08389(2)	-0.15020(2)	0.36491(3)	0.0079(1)	0.0099(2)	0.0070(2)	0.0070(2)	0.0014(1)	0.0006(1)	0.0003(1)
X(1)	40.3(1)	¾	¼	¼	0.0092(2)	0.0137(3)	0.0080(2)	0.0058(2)	0	0	0
X(2)	161.7(2)	-0.19038(2)	0.04495(2)	0.37987(2)	0.0101(1)	0.0096(1)	0.0119(1)	0.0087(1)	0.0016(1)	-0.0011(1)	0.0001(1)
X(3)	165.3(3)	-0.10090(2)	-0.17893(2)	0.89483(3)	0.0175(1)	0.0131(1)	0.0160(2)	0.0234(2)	0.0004(1)	-0.0044(1)	-0.0023(1)
X(4)	20.4(1)	¾	¾	0.14318(9)	0.0105(3)	0.0087(3)	0.0087(3)	0.0142(6)	0	0	0
Y(1)	21.7(1)	¾	¾	0.05586(11)	0.0188(4)	0.0102(4)	0.0102(4)	0.0359(8)	0	0	0
Y(2)	54.7(2)	0	0	0	0.0091(2)	0.0076(3)	0.0078(3)	0.0118(3)	0.0005(2)	-0.0002(2)	-0.0009(2)
Y(3)	121.6(2)	-0.11165(2)	0.12018(2)	0.12789(3)	0.0094(1)	0.0101(2)	0.0100(2)	0.0081(2)	0.0007(1)	0.0004(1)	-0.0004(1)
T(1)	10.43(6)	0.05304(14)	0.05304(14)	¼	0.0183(10)	0.0217(13)	0.0217(13)	0.0115(15)	-0.0066(12)	-0.0089(9)	0.0089(9)
T(2)	4.64(8)	¼	¼	¼	0.0100						
O(1)		-0.21994(6)	0.17280(6)	0.08462(8)	0.0107(2)	0.0140(4)	0.0092(4)	0.0090(4)	0.0000(3)	-0.0005(3)	0.0008(3)
O(2)		-0.12070(6)	0.16054(6)	0.28284(8)	0.0127(2)	0.0166(5)	0.0102(4)	0.0113(4)	-0.0002(3)	-0.0046(4)	0.0014(3)
O(3)		-0.04282(6)	0.22472(6)	0.07802(8)	0.0133(2)	0.0173(5)	0.0126(4)	0.0101(4)	0.0056(4)	0.0029(4)	0.0020(3)
O(4)		-0.06177(6)	0.10461(6)	0.47133(8)	0.0103(2)	0.0122(4)	0.0097(4)	0.0091(4)	0.0004(3)	-0.0018(3)	0.0008(3)
O(5)		-0.17148(6)	0.01169(6)	0.17953(8)	0.0117(2)	0..0119(4)	0.0131(4)	0.0101(4)	0.0048(3)	0.0004(3)	-0.0014(3)
O(6)		-0.12105(6)	-0.27629(6)	0.05351(9)	0.0148(2)	0.0190(5)	0.0122(4)	0.0133(5)	0.0021(4)	0.0023(4)	0.0053(4)
O(7*A*)	32.0(5)	0.05565(14)	0.1760(2)	0.3201(2)	0.0102(7)						
O(7*B*)	32.0(5)	0.0445(2)	0.1466(3)	0.3069(2)	0.0172(7)						
O(8)		-0.06037(6)	-0.09201(6)	0.06654(8)	0.0099(2)	0.0089(4)	0.0093(4)	0.0114(4)	0.0018(3)	0.0017(3)	-0.0003(3)
O(9)		-0.14607(6)	-0.14607(6)	¼	0.0124(3)	0.0136(4)	0.0136(4)	0.0099(6)	-0.0018(5)	-0.0015(4)	0.0015(4)
O(10)	10.6(2)	¾	¾	0.8700(3)	0.0305(13)	0.0317(15)	0.0317(15)	0.0279(23)	0	0	0
O(11*A*)	31(3)	-0.0030(2)	0.0628(4)	0.1351(9)	0.0079(10)						
O(11*B*)	33(3)	-0.0013(2)	0.0536(4)	0.1543(9)	0.0109(8)						
O(12)	11.2(2)	0.1772(5)	0.2733(4)	0.2044(6)	0.0263(19)						
H(2)	0.9(1)	¼	¼	0.2070	0.0200						

Note: $U_{(eq)}$ is defined as one third of the trace of the orthogonalized U_{ij} tensor.
[a] The exponent of the anisotropic displacement factor takes the form: $-2\pi^2 [h^2 a^{*2} U_{11} + ... + 2 h k a^* b^* U_{12}]$.
[b] ss = observed site-scattering, in electrons per formula unit (*epfu*).

cement parameters at both the *O*(7) and *O*(11) sites, each split into two positions [see Fig. 3 for details of the electron density at the *O*(7) sites], as already observed by Groat *et al*. (1994). Occupancy for each split site was constrained to be complementary, but no constraint on the occupancy of the *O*(7) and *O*(11) sites was applied. Isotropic displacement parameters were refined for both split sites. A separation *O*(11*A*)–*O*(11*B*) of 0.23 Å and *O*(7*A*)–*O*(7*B*) of 0.52 Å was obtained at convergence, in agreement with the findings of Groat *et al*. (1994). Thus, our model depicts a local environment with large vacant *T*(1) tetrahedral cavities formed by two *O*(7*A*) and two *O*(11*A*) anions, and smaller occupied tetrahedral *T*(1) sites coordinated by two *O*(7*B*) and O(11*B*) sites. Our refinement yielded a site occupancy complementary for *O*(7)B and *O*(11*B*), compatible with half occupancy of *T*(1) sites (Table 3). Following Groat *et al*. (1994, 1996), the *T*(1) sites can be occupied by B and Al. The observed mean bond-length (<^{IV}*T*(1)–O(B)> 1.514 Å) is rather large for full occupancy by boron (<^{IV}B–O> 1.47 Å; Shannon 1976) and too short for full occupancy by aluminum (<^{IV}Al–O> 1.75 Å; Shannon 1976). Therefore, most of the scattering at *T*(1) must be due to B. In terms of the observed site-scattering values (10.43 *epfu*), we estimate 2.09 *apfu* of B at *T*(1). However, this value is probably underestimated because some of the electron density near the *T*(1) site was still present in the difference-Fourier maps.

The *T*(2) site lies between two *O*(10) anions along the channels parallel to the *c* crystallographic axis. In B-bearing vesuvianite, H at this site [*i.e.*, *H*(2)] is partially or totally replaced by B. One additional partially occupied oxygen atom [*O*(12)] around the *T*(2) site is observed in X-ray-diffraction data in cases where B enters at the *T*(2) site (Groat *et al*. 1994, 1996). In this case, the coordination at the *T*(2) sites is a matter of debate. Groat *et al*. (1996) have proposed a mixed coordination model for B at the *T*(2) sites in B-rich vesuvianite. On the basis of the observed site-scattering values and short-range order, those authors proposed that most of the B at *T*(2) has planar 3-fold coordination [with one *O*(10) site vacant and only two of the eight possible *O*(12) sites occupied], whereas some B has linear coordination with two *O*(10) anions. In our model, the site occupancy of the *T*(2) and *O*(12) sites has been refined using the scattering curve of B and O^{2-}, respectively. These two sites were refined considering isotropic displacement parameters, and the value of *T*(2) was fixed at 0.01 Å^2. At convergence, a residual maximum was found at a distance of 0.9 Å from *O*(10)

TABLE 4. SELECTED BOND-LENGTHS (Å) AND GEOMETRICAL PARAMETERS FOR WILUITE FROM ARICCIA, LATIUM, ITALY

Z(1)-*O*(1)[a]	×4	1.636(1)	*Y*(1)-*O*(6)[n]	×4	2.069(1)	*X*(1)-*O*(1)[b]	×4	2.333(1)
Vol. (Å³)		2.239	*Y*(1)-O(10)[c]		2.176(4)	*X*(1)-*O*(2)[o]	×4	2.501(1)
TAV		9.665	<*Y*(1)-*O*>		2.090	<*X*(1)-*O*>		2.417
TQE		1.002						
			Y(2)-O(4)[g]	×2	1.939(1)	*X*(2)-O(1)[n]		2.489(1)
Z(2)-*O*(2)[g]		1.631(1)	*Y*(2)-O(8)	×2	1.897(1)	*X*(2)-O(2)		2.406(1)
Z(2)-*O*(3)[e]		1.628(1)	*Y*(2)-O(11*A*)	×2	1.865(6)	*X*(2)-O(3)[d]		2.381(1)
Z(2)-O(4)[d]		1.670(1)	*Y*(2)-O(11*B*)	×2	1.993(7)	*X*(2)-O(4)		2.472(1)
Z(2)-O(7*A*)[d]		1.667(2)	<*Y*(2)-*O*,O(11*A*)>		1.900	*X*(2)-O(5)		2.421(1)
Z(2)-O(7*B*)[d]		1.652(2)	Vol. (Å³)		9.041	*X*(2)-O(5)[h]		2.339(1)
<*Z*(2)-*O*,O(7*A*)>		1.649	OAV		26.618	*X*(2)-O(8)[g]		2.350(1)
Vol (Å³)		2.252	OQE		1.008	<*X*(2)-*O*>		2.408
TAV		59.021	<*Y*(2)-*O*,O(11*B*)>		1.943			
TQE		1.015	Vol. (Å³)		9.731	*X*(3)-O(3)[i]		2.392(1)
<*Z*(2)-*O*,O(7*B*)>		1.645	OAV		9.409	*X*(3)-O(6)[i]		2.427(1)
Vol. (Å³)		2.255	OQE		1.004	*X*(3)-O(6)[m]		2.829(1)
TAV		37.232				*X*(3)-O(7*A*)[d]	×½	2.431(2)
TQE		1.009	*Y*(3)-O(1)		1.959(1)	*X*(3)-O(7*B*)[d]	×½	2.457(2)
			Y(3)-O(2)		1.927(1)	*X*(3)-O(7*A*)[i]	×½	2.614(2)
Z(3)-O(5)[g]		1.624(1)	*Y*(3)-O(3)		2.052(1)	*X*(3)-O(7*A*)[j]	×½	2.573(2)
Z(3)-O(6)[f]		1.609(1)	*Y*(3)-O(4)[p]		2.052(1)	*X*(3)-O(7*A*)[k]	×½	2.543(4)
Z(3)-O(8)[g]		1.629(1)	*Y*(3)-O(5)		2.039(1)	*X*(3)-O(7*B*)[k]	×½	3.060(5)
Z(3)-O(9)		1.664(1)	*Y*(3)-O(11*A*)	×½	1.934(5)	*X*(3)-O(8)[j]		2.512(1)
<*Z*(3)-*O*>		1.631	*Y*(3)-O(11*B*)	×½	2.049(6)	*X*(3)-O(10)[l]		2.612(1)
Vol. (Å³)		2.221	<*Y*(3)-*O*,O(11*A*)>		1.994	*X*(3)-O(11*A*)[j]	×½	2.474(6)
TAV		9.024	Vol. (Å³)		10.414	*X*(3)-O(11*B*)[j]	×½	2.606(7)
TQE		1.002	OAV		31.975	*X*(3)-O(12)[k]		2.640(7)
			OQE		1.010	<*X*(3)-*O*,*OA*>		2.516
T(1)-O(7*A*)	×2	2.100(4)	<*Y*(3)-*O*,O(11*B*)>		2.013	<*X*(3)-*O*,*OB*>		2.587
T(1)-O(7*B*)	×2	1.620(5)	Vol. (Å³)		10.796			
T(1)-O(11*A*)	×2	1.615(10)	OAV		16.395	*X*(4)-O(6)[n]	×4	2.319(1)
T(1)-O(11*B*)	×2	1.408(9)	OQE		1.005	*X*(4)-O(9)[c]	×4	2.627(1)
<*T*(1)-O(*A*)>		1.858				<*X*(4)-*O*>		2.473
Vol. (Å³)		3.054	*T*(2)-O(10)[q]		1.404(4)			
<*T*(1)-O(*B*)>		1.514	*T*(2)-O(12)	×2	1.315(7)	*H*(2)-O(10)[q]		0.901(4)
Vol. (Å³)		1.725	<*T*(2)-*O*>		1.345			

Equivalent positions: a: y + ½, –x, –z; b: x + 1, y, z; c: –x + ½, –y + ½, z; d: –y, –x, z + ½; e: y–½, –x, –z + 1; f: x, –y–½, –z + ½; g: y, x, –z + ½; h: –x–½, y, –z + ½; i: –x, –y, –z + 1; j: x, y, z + 1; k: –x, y–½, z + ½; l: x–1, y–1, z; m: –y–½, x, z + 1; n: –y + ½, x + 1, z; o: x, y, z–1; p: –y, –x, z–½; q: –x + 1, –y + 1, –z + 1.
TAV: Tetrahedral angle variance; TQE: tetrahedral quadratic elongation; OAV: octahedral angle variance; OQE: octahedral quadratic elongation (Robinson *et al.* 1971). Sample number: 26FB.

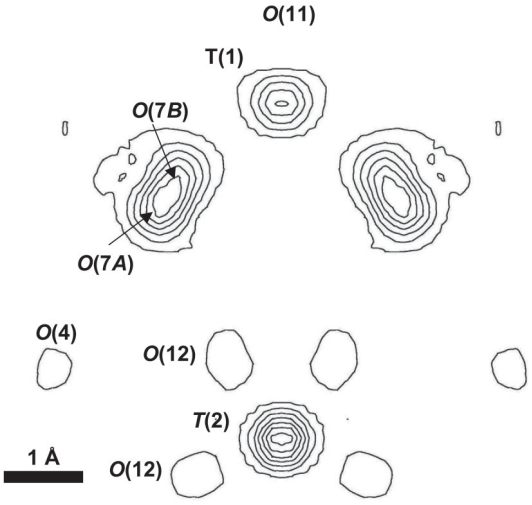

FIG. 3. The shape of the electron density at the *T*(1) and *T*(2) sites showing disorder at the *O*(7) and *T*(1) sites. The *O*(11) sites are out-of-plane aligned with *T*(1) and *T*(2). Contours at 2 e^-. Difference-Fourier map projected onto the (2$\bar{2}$3) plane; contour lines in steps of 2 e^-Å^{-3} starting from 2 e^-Å^{-3}.

with atom coordinates very close to those of Lager *et al.* (1999) for the *H*(2) site [the observed *z*/*c* coordinate of *H*(2) is 0.293, in agreement with the value 0.28 reported by Lager *et al.* 1999]. Therefore, this atom position was added to the model, which fixed the site coordinates and the isotropic displacement parameter at 0.02 Å^2. The refined site-scattering value at *T*(2) is compatible with nearly full occupancy by B. This being the case, we should observe site occupancies 0.25 for *O*(12) and 0.5 for *O*(10). However, the refined site-occupancies are 0.17 and 0.66, respectively. This finding is compatible with a 32% occupancy by H and 68% occupancy by B at *T*(2), yielding a lower site-scattering value than observed (3.72 *epfu versus* 5.08 *apfu* observed). Owing

TABLE 6. CRYSTAL-CHEMICAL FORMULA AND AGREEMENT BETWEEN OBSERVED AND CALCULATED SITE-SCATTERING VALUES FOR WILUITE FROM ARICCIA, LATIUM, ITALY

$^{X}(Ca_{1.72}Mg_{0.18}Sr_{0.02}La_{0.08}Ce_{0.04}Nd_{0.01})\ ^{Y(1)}(Fe^{3+}_{0.36}Mg_{0.26}Ti_{0.27}Mn_{0.11})$
$^{Y(2)}(Al_{3.67}Fe^{3+}_{0.19}Mg_{0.14})\ ^{Y(3)}(Al_{3.29}Fe^{3+}_{1.36}Mg_{3.35})$
$^{T(1)}(B_{2.18}Al_{0.02}Be_{0.02}H_{0.47}\square_{1.31})\ ^{T(2)}(B_{0.68}H_{0.32})\ ^{Z}Si_{18}O_{68}\ ^{O(11)}(F_{1.21}O_{6.79})\ ^{[O(10)+O(12)]}O_{2.68}$

Site-scattering values, in *epfu*

$T(1) + T(2)_{obs}$	15.07	Y_{obs}	198.0	X_{obs}	387.7
$T(1) + T(2)_{calc}$	15.47	Y_{calc}	193.8	X_{calc}	383.3
Difference (%)	2.6	Difference (%)	2.1	Difference (%)	1.1

The observed values are obtained from the structure refinement, whereas the calculated values are derived from results of chemical analyses. Values are expressed in electrons per formula unit (*epfu*).

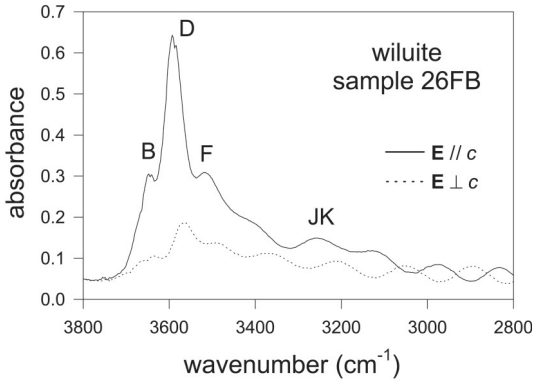

FIG. 4. Polarized absorption spectra of wiluite 26FB in the principal OH-stretching region. Section parallel to (100), thickness 18 μm.

to the difficulty in accounting for a model with two weak scatterers at a distance of only 0.5 Å, the observed site-scattering value at *T*(2) may be overestimated. Moreover, Lager *et al.* (1999) found a large value of root-mean-square (RMS) displacement associated with *H*(2) in room-temperature neutron-diffraction data, and interpreted this feature as due to disorder of the *H*(2) atom. The IR spectrum discussed in the next section shows that there is some disordered H at the *H*(2) sites, as indicated by the weak and broad *JK* absorption bands. Considering triangular coordination for B at *T*(2), the observed mean bond-length (1.344 Å) is shorter than expected for B in this coordination (1.37 Å), but still in good agreement considering the error associated with the coordinates of the *O*(12) site.

INFRARED SPECTROSCOPY

Single-crystal, polarized-light spectra were collected on a section 18-mm-thick oriented parallel to (100), using a Perkin Elmer FTIR 1760X spectrophotometer, equipped with Olympus IR microscope, a nitrogen-cooled MCT detector, and a golden wire AgBr polarizer. The OH-stretching FTIR spectrum (Fig. 4) invariably consists of a rather well-defined triplet of broad bands labeled B (3639 cm^{-1}), *D* (3573 cm^{-1}) and *F* (3488 cm^{-1}) (the band notation used here is from Groat *et al.* 1995) and a very broad, composite absorption at 3300 cm^{-1} (*JK* in Fig. 4). This pattern is characteristic of B-bearing vesuvianite (*e.g.*, Groat *et al.* 1995, Bellatreccia *et al.* 2004). Figure 4 also shows that all bands are strongly polarized, with maximum absorption for **E** // *c* and minimum absorption for **E** ⊥ **c**. This polarization behavior is in full agreement with the findings of Groat *et al.* (1995), and supports the assignment of the higher-frequency *B*, *D* and *F* triplet of bands to the *O*(11)–*H*(1) dipole, and the assignment of the lower-frequency broad absorption *JK* to the *O*(10)–*H*(2) dipole (Bellatreccia *et al.* 2004).

The quantitative determination of H_2O (c, in wt.%) in minerals by IR spectroscopy is based on the Lambert–Beer law: $c = a_i / (\varepsilon_i * D)$, where a_i is the integrated absorption coefficient measured from the IR spectrum, D is the density, and ε_i is the matrix-specific integral molar absorptivity, in $l^* mol^{-1} * cm^{-2}$ (Beran *et al.* 1993, Libowitzky & Rossman 1997). For vesuvianite, ε_i has been recently calibrated by Bellatreccia *et al.* (2005) for a large number of B-bearing samples. For wiluite from Ariccia $\varepsilon_i = 9 \pm 1.5 \times 10^4\ l^* mol^{-1} * cm^{-2}$ is calculated from the IR spectrum using the H_2O content established by SIMS (0.239 wt.% H_2O, Table 1). As shown by Bellatreccia *et al.* (2005), this value is in excellent agreement with the curve of Libowitzky & Rossman (1997).

The spectra collected in the 1600–1100 cm^{-1} region (Fig. 5) show several sharp bands with distinct pleochroic behavior. This region is poorly studied; however, it is known (*e.g.*, Ross 1974) that the most significant B–O absorptions occur in this range. In particular, the stretching vibrations of the BO_3 group are characteristically found at higher frequency (1400–1200 cm^{-1}), whereas the stretching vibrations of the BO_4 group are observed at lower frequency (<1200 cm^{-1}), thus partly overlapping the Si–O stretching bands (Grew & Rossman 1985). The BO_3 group in the vesuvianite structure is oriented with the longer B–*O*(10) bond parallel to the *c* axis; therefore, the polarization behavior shown in Figure 5 suggests the assignment of the 1267 cm^{-1} band to this bond, and the assignment of the 1370 cm^{-1} absorption to the two equivalent, and slightly shorter (1.40 *versus* 1.32 Å: Table 4) B–O(12) bonds. Assignment of the 1418 and 1472 cm^{-1} bands (Fig. 5) is unclear at the moment. A reasonable possibility involves the combination of lower-frequency bands. Alternatively, these bands could be related to the presence in the structure of a minor proportion of CO_3 groups; however, at present we do not have data to support (or dismiss) this possibility. The absorption at 1110 cm^{-1}

can be assigned to the vibration of BO_4 groups (Grew & Rossman 1985). Note that this band is not polarized in the (100) plane. This band can be confidently assigned to the shorter *T*(1)–*O*(11) bonds (Table 4). Additional $^{[4]}$B–O bands are expected in the spectrum at lower frequency, but these totally overlap the more intense Si–O region and cannot be resolved.

X-Ray Absorption Fine Structure Spectroscopy (XAFS)

Vesuvianite-group minerals are known to host their non-tetrahedrally-coordinated cations in four types of sites, which have, respectively, a coordination of eight (*X*), five [*Y*(1)], and six [*Y*(2) and *Y*(3)]. Whereas the eight-fold occupancy of such large *X* cations as Ca, Sr and the REE is well established, and the six-fold preference of the small Al, Ti and Fe^{3+} cations for the two *Y*(2) and *Y*(3) sites is also confirmed (Groat *et al*. 1996), there is still disagreement about the distribution of the divalent cations (Mg, Mn, and Fe^{2+}). This question is especially interesting for wiluite, where divalent cations are involved in the entry of B at the tetrahedral *T*(1), *T*(2) sites. We addressed this problem by considering that (1) in the sample of wiluite studied, Mg is distributed over all three *Y*(1), *Y*(2), *Y*(3) sites, the latter being its preferred site (Table 6), and (2) the *Y*(1) site, by itself unusual for being in the rare square-pyramidal configuration in vesuvianite-group minerals (Coda *et al*. 1970), in our wiluite undergoes a further distortion, from squat to elongate [Table 4; see also Ohkawa *et al*. (1992) for comparison with vesuvianite]. Another major structural change is that in wiluite, the *Y*(3) and *Y*(2) octahedra contain divalent cations, thus forming continuous zigzag chains, whereas in vesuvianite, the small *Y*(2) octahedra contain only Al (Lager *et al*. 1999). In order to evaluate the distribution of divalent cations in wiluite, we selected Mg in preference to Fe for two major reasons: (1) Mg is significantly more abundant, and is always divalent, whereas a substantial fraction of the Fe present is in the trivalent state, which makes it prefer six-fold coordination; (2) the resolution of our technique at the Mg *K*-edge energy is greater than at the Fe *K*-edge energy. Furthermore, to cross-check the results for divalent Mg, we determined the coordination environment for Al, a cation that is only trivalent and assigned to the *Y*(3) and *Y*(2) octahedra, based on the results of the structure refinement.

The technique we used is X-ray absorption fine structure spectroscopy (XAFS), which is well known to be chemically selective, thus giving unequivocal information on each atom present in such complex chemical compounds. The spectra were recorded at the soft X-ray beam line SB03–3 of the SSRL facility, at 3 GeV and *ca*. 65 mA ring current; we used a (400) YB_{66} double-crystal monochromator, which yields an experimental resolution of *ca*. 0.4–0.5 eV, in the total yield (TEY) mode, with the powdered samples scanned at 0.3 eV steps for 5 s and set at a 35° angle from the beam forward direction. We normally record our spectra in the near *K*-edge region (XANES, X-ray absorption near-edge structure), namely, in the energy range 1280–1400 eV for Mg, and in the 1540–1620 eV interval for Al. Both ranges encompass the various subregions of the

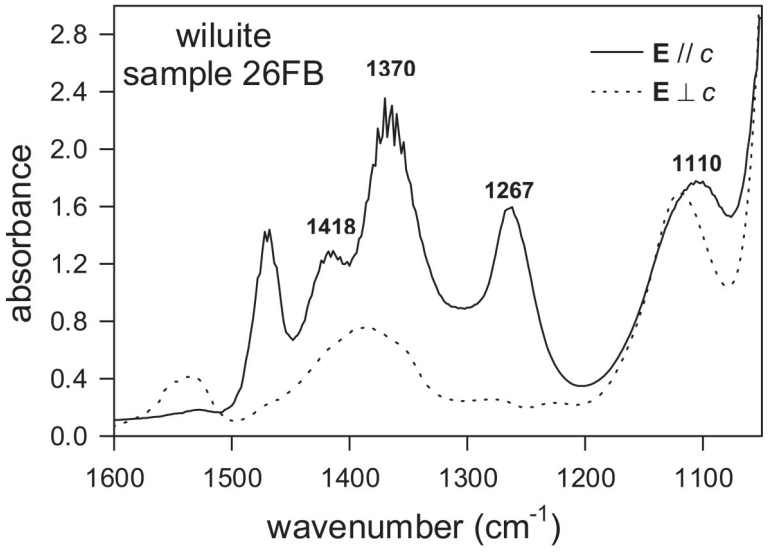

FIG. 5. Polarized absorption spectra of wiluite 26FB in the 1600–1100 cm^{-1} region. Section parallel to (100), thickness 18 mm.

edge (Mottana 2004) and provide a good enough resolution while being wide enough to pinpoint all subtle spectral features. The spectrum of vesuvianite from Pitigliano (sample 10FB, Bellatreccia *et al.*, unpubl. data) recorded for comparison, is displayed in Figure 6. Experimental spectra were first energy-corrected as a function of the ring current, then fitted with a Victoreen polynomial function to account for the baseline and normalized to 1 at high energy. The observed features were carefully located using algorithms able to detect changes in the peak signal of the order of 10^{-3}–10^{-4} and are believed to be accurate to ±0.1 eV in energy and ±5 relative % in intensity.

The Mg XANES spectrum of wiluite (Fig. 6a) consists of a single, broad feature B centered at 1311.3 eV, clearly the convolution of several contributions, which suggests that Mg is distributed over a variety of sites that differ primarily in shape rather than local energy. By contrast, the spectrum of vesuvianite, although of lesser quality because of the increased background-noise, shows two clearly resolved features; the low-energy one (A) is fairly sharp and probably unique, whereas the high-energy one (B) is clearly the convolution of two or more contributions. Such convoluted spectra are not easy to assign, but we confidently suggest that feature A at 1308.4 eV in vesuvianite is generated by five-fold coordinated Mg, and the superimposed B + C features at 1311.3 eV by the six-fold coordinated site. Thus we also attribute shoulder A on the rising limb of the composite edge to Mg located in the *Y*(1) elongate pyramidal site, whereas we attribute the broad peak B with its high-energy shoulder C to six-fold coordinated Mg located at the *Y*(2) and *Y*(3) sites. Magnesium at the latter site is probably responsible for the strong intensity of B, at least according to the cation assignment resulting from the structure refinement (*cf.* Table 6).

The Al XANES spectra of wiluite and vesuvianite (Fig. 6b) consist of two major, partially superimposed absorption-peaks A (1566.8 eV) and B (1569.7 eV), followed by three minor ones, which are barely discernible in the background because of the low Al bulk content of both samples. The patterns are typical for Al in octahedral coordination, as in grossular and polylithionite (Mottana *et al.* 1997). A faint shoulder at 1564.1 (arrow) is present in both samples, which hints at the presence of $^{[4]}$Al. However, such a contribution, if any, is ≤5% Al_{tot}. The two spectra are nearly identical in their energies, thus suggesting that Al is located in the same environments in both minerals. However, they differ somewhat in their intensities, which suggests a slightly more disordered distribution of Al in wiluite than in vesuvianite.

Conclusions

We describe the occurrence of the rare silicoborate wiluite from the tephra of the Alban Hills volcano,

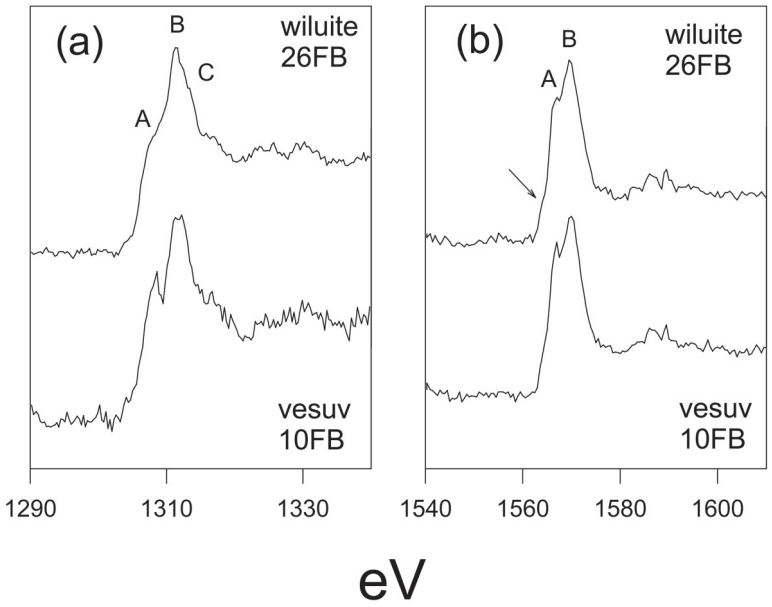

FIG. 6. XAFS spectra of wiluite 26FB (this work) and vesuvianite 10FB (Bellatreccia *et al.*, unpubl. data) in the regions of (a) the Mg *K*-edge and (b) the Al *K*-edge, respectively.

Roman comagmatic region. The main conclusions of this study are:

1) The sample studied is uniaxial (+), and shows anomalous extinction.

2) According to EMPA + SIMS data, wiluite from Ariccia has a composition very similar to that of holotype wiluite from the Sakha Republic (Groat *et al*. 1998), but it has significantly higher B and F contents.

3) Both X-ray structure refinement and polarized IR spectroscopy show that B is present both in tetrahedral and triangular coordination, although at present neither technique can provide conclusive quantitative data on the B speciation between these configurations.

4) The OH-stretching FTIR spectrum is characteristic of a B-bearing vesuvianite-group mineral; the integrated molar absorption-coefficient calculated from the polarized-light IR spectrum and SIMS analysis of wiluite for H_2O is $\varepsilon_i = 9 \pm 1.5 \times 10^4$ l* mol^{-1}* cm^{-2}.

5) Our XAS results confirm the presence of Mg in at least three coordination environments, including the unusual five-fold elongate pyramidal site, whereas Al is in the octahedrally coordinated sites, which are slightly more disordered in wiluite than in vesuvianite.

Acknowledgements

Part of this work was done during the stay of FB at the Marie Curie training site, Institut für Mineralogie und Kristallographie, Universität Wien (Austria), financed by the European Commission, contract number HPMT–CT–2000–00138. Thanks are due to G. Giester, U. Kolitsch, A. Beran and E. Libowitzky, Institut für Mineralogie und Kristallographie, Universität Wien for the single-crystal and micro-IR data collection. Marcello Serracino assisted with the EMP analyses. The National Research Council of Italy (CNR) is acknowledged for funding the SIMS laboratory at IGG (Pavia). The suggestions of Lee Groat and an anonymous referee helped to improve the clarity of the paper. We are very happy to dedicate this article to Michael E. Fleet in recognition of his work on the crystal chemistry of boron.

References

Anders, E. & Ebihara, M. (1982): Solar-system abundances of the elements. *Geochim. Cosmochim. Acta* **46**, 2263-2380.

Bellatreccia, F. (2003): *La Cristallochimica delle Vesuvianiti*. Ph.D. thesis, Università di Roma La Sapienza, Roma, Italia.

_____, Della Ventura, G., Ottolini, L., Libowitzky, E. & Beran, A. (2005): The quantitative analysis of OH in vesuvianite: a polarized FTIR and SIMS study. *Phys. Chem. Minerals* **78**, 65-76.

Beran, A., Langer, K. & Andrut, M. (1993): Single crystal infrared spectra in the range of OH fundamentals of paragenetic garnet, omphacite and kyanite in an eclogitic mantle xenolith. *Mineral. Petrol.* **48**, 257-268.

Borovikova, E.Yu., Kurazhkovskaya, V.S. & Alferova, M.S. (2003): Infrared spectra and factor group analysis of vesuvianites in OH region. *Int. Symp. on Light Elements in Rock-Forming Minerals* (*LERM 2003*), *Abstr.*, 8.

Coda, A., Della Giusta, A., Isetti, G. & Mazzi, F. (1970): On the crystal structure of vesuvianite. *Atti Accad. Sci. Torino* **105**, 63-84.

Deer, W.A., Howie, R.A. & Zussman, J. (1982): *Rock-Forming Minerals*. **1A**. *Orthosilicates*. Longmans, Green and Co., London, U.K.

Della Ventura, G., Bellatreccia, F. & Williams, C.T. (1999): Zr- and *LREE*-rich titanite from Tre Croci, Vico Volcanic complex (Latium, Italy). *Mineral. Mag.* **63**, 123-130.

_____, Mottana, A., Parodi, G.C., Raudsepp, M., Bellatreccia, F., Caprilli, E., Rossi, P. & Fiori, S. (1996): Monazite–huttonite solid-solutions from the Vico Volcanic Complex, Latium, Italy. *Mineral. Mag.* **60**, 751-758.

_____, Parodi, G.C., Mottana, A. & Chaussidon, M. (1993): Peprossiite-(Ce), a new mineral from Campagnano (Italy): the first anhydrous rare-earth-element borate. *Eur. J. Mineral.* **5**, 53-58.

Federico, M., Peccerillo, A., Barbieri, M. & Wu, T.W. (1994): Mineralogical and geochemical study of granular xenoliths from the Alban Hills volcano, central Italy, bearing on evolutionary processes in potassic magma chambers. *Contrib. Mineral. Petrol.* **115**, 384-401.

Fitzgerald, S., Leavens, P.B., Rehingold, A.L. & Nelen, J.A. (1987): Crystal structure of a *REE*-bearing vesuvianite from San Benito County, California. *Am. Mineral.* **72**, 625-628.

Giordano, G., De Rita, D., Cas, R.A. & Rodani, S. (2002): Valley pond and ignimbrite veneer deposits in the small-volume phreatomagmatic "Peperino Albano" basic ignimbrite, Lago Albano maar, Colli Albani volcano, Italy: influence of topography. *J. Volcanol. Geotherm. Res.* **118**, 131-144.

Grew, E.S. & Rossman, G.R. (1985): Co-ordination of boron in sillimanite. *Mineral. Mag.* **49**, 132-135.

Groat, L.A., Hawthorne, F.C. & Ercit, T.S. (1992): The chemistry of vesuvianite. *Can. Mineral.* **30**, 19-48.

_____, _____ & _____ (1994): The incorporation of boron into the vesuvianite structure. *Can. Mineral.* **32**, 505-523.

_____, _____, _____ & Grice. J.D. (1998): Wiluite, Ca_{19} (Al,Mg,Fe,Ti)$_{13}$ (B,Al,□)$_5$ $Si_{18}O_{68}$(O,OH)$_{10}$, a new mineral species isostructural with vesuvianite, from

the Sakha Republic, Russian Federation. *Can. Mineral.* **36**, 1301-1304.

_____, _____, LAGER, G.A., SCHULTZ, A.J. & ERCIT, T.S. (1996): X-ray and neutron crystal-structure refinements of a boron-bearing vesuvianite. *Can. Mineral.* **34**, 1059-1070.

_____, _____, ROSSMAN, G.R. & ERCIT, T.S. (1995): The infrared spectroscopy of vesuvianite in the OH region. *Can. Mineral.* **33**, 609-626.

HAHN, T., ed. (1995): *International Tables for Crystallography* **A**. Kluwer Academic Publishers, Dordrecht, The Netherlands.

HURLBUT, C.S., JR. (1984): The jeweler's refractometer as a mineralogical tool. *Am. Mineral.* **69**, 391-398.

LAGER, G.A., XIE, QIANYEN, ROSS, F.K., ROSSMAN, G.R., ARMBRUSTER, T., ROTELLA, F.J. & SCHULTZ, A.J. (1999): Hydrogen-atom position in *P*4/*nnc* vesuvianite. *Can. Mineral.* **37**, 763-768.

LIBOWITZKY, E. & ROSSMAN, G.R. (1997): An IR absorption calibration for water in minerals. *Am. Mineral.* **82**, 1111-1115.

MOTTANA, A. (2004): X-ray absorption spectroscopy in mineralogy: theory and experiment in the XANES region. *Eur. Mineral. Union, Notes in Mineralogy* **6**, 465-552.

_____, ROBERT, J.-L., MARCELLI, A., GIULI, G., DELLA VENTURA, A., PARIS, E. & WU, Z.Y. (1997): Octahedral *versus* tetrahedral coordination of Al in synthetic micas determined by XANES. *Am. Mineral.* **82**, 497-502.

OBERTI, R., OTTOLINI, L., CÁMARA, F. & DELLA VENTURA, G. (1999): Crystal structure refinement of non-metamict Th-rich hellandite-(Ce) from Latium (Italy) and crystal chemistry of the hellandite-group minerals. *Am. Mineral.* **84**, 913-921.

OHKAWA, M., YOSHIASA, A. & TAKENO, S. (1992): Crystal chemistry of vesuvianite: site preferences of square-pyramidal coordinated sites. *Am. Mineral.* **77**, 945-953.

OTTOLINI, L., CÁMARA, F., HAWTHORNE, F.C. & STIRLING, J. (2002): SIMS matrix effects in the analysis of light elements in silicate minerals: comparison with SREF and EMPA data. *Am. Mineral.* **87**, 1477-1485.

_____ & OBERTI, R. (2000): Accurate quantification of H, Li, Be, B, F, Ba, REE, Y, Th, and U in complex matrixes: a combined approach based on SIMS and single-crystal structure refinement. *Anal. Chem.* **72**, 3731-3738.

OTWINOWSKI, Z. & MINOR, W. (1997): Processing of X-ray diffraction data collected in oscillation mode. *In* Macromolecular Crystallography A (C.W. Carter, Jr. & R.M. Sweet, eds.). Academic Press, New York, N.Y. (307-326).

PECCERILLO, A., POLI, G. & TOLOMEO, L. (1984): Genesis, evolution and tectonic significance of K-rich volcanics from the Alban Hills (Roman comagmatic region) as inferred from trace element geochemistry. *Contrib. Mineral. Petrol.* **86**, 230-240.

POUCHOU, J.L. & PICHOIR, F. (1985): 'PAP' $\phi(\rho Z)$ procedure for improved quantitative micro-analysis. *In* Microbeam Analysis (J.T. Armstrong, ed.). San Francisco Press, San Francisco, California (104–106).

ROBINSON, K., GIBBS, G.V. & RIBBE, P.H. (1971): Quadratic elongation: a quantitative measure of distortion in coordination polyhedra. *Science* **172**, 567-570.

ROSS, S.D. (1974): Borates. *In* The Infrared Spectra of Minerals (V.C. Farmer, ed.). The Mineralogical Society, London, U.K. (205-226).

SHANNON, R.D. (1976): Revised affective ionic radii and systematic studies of interatomic distances in halides and chalcogenides. *Acta Crystallogr.* **A32**, 751–767.

SHELDRICK, G. M. (1997): SHELX–97. *Program for Crystal Structure Refinement*. Univerity of Göttingen, Göttingen, Germany.

WILSON, A.J.C., ed. (1995): *International Tables for Crystallography* **C**. Kluwer Academic Publishers, Dordrecht, The Netherlands.

Received July 16, 2004, revised manuscript accepted June 14, 2005.